Available online at www.sciencedirect.com

Journal of Nuclear Materials 358 (2006) 235–242

journal of nuclear materials

www.elsevier.com/locate/jnucmat

Hydrogen permeability through a mixed molten salt of LiF, NaF and KF (Flinak) as a heat-transfer fluid

Satoshi Fukada *, Akio Morisaki

Department of Applied Quantum Physics and Nuclear Engineering, Kyushu University, 6-10-1 Hakozaki, Higashi-ku, Fukuoka 812-8581, Japan

Received 10 March 2006; accepted 6 July 2006

Abstract

Permeability, diffusivity and solubility of hydrogen in Flinak, a mixed molten salt of LiF (46.5%), NaF (11.5%) and KF (42%), were determined using a vessel supported by a Ni plate. Diffusion-limiting permeation was confirmed by experimental data where hydrogen permeation rates were in reverse proportion to the thickness of Flinak. Diffusivities determined in the range of 500–750 °C were correlated to an Arrhenius equation with the activation energy of 50 kJ/mol. Since the dependence of hydrogen solubility in Flinak on pressure was almost linear, hydrogen was dissolved as H_2 in Flinak. The H_2 solubility in Flinak was correlated to a Henry law, and its solubility constant was discussed in terms of macroscopic surface tension and unspecified interaction energy between the molten salt and dissolved gaseous molecules.

PACS: 61.20.Qg; 66.10.Cb

1. Introduction

Flinak is a mixed molten salt comprising LiF, NaF and KF that was previously investigated as a heat-transfer fluid of a molten salt nuclear reactor [1]. This is because Flinak is stable at higher temperatures and because of moderate specific heat and sufficient thermal conductivity. A mixture of 46.5 (LiF), 11.5 (NaF) and 42 (KF) in mole% has the lowest melting temperature of 454 °C [2]. Recently, Flinak is proposed also as a secondary heat-transfer fluid of an advanced high-temperature nuclear reactor of Generation IV [3]. Reactors are designed to produce H_2 using nuclear heat at higher temperatures. In addition, there is possibility in applying Flinak to the secondary fluid of a Flibe ($2LiF + BeF_2$ mixed molten salt) self-cooled nuclear fusion reactor [4–6]. Use of Flinak as secondary heat-transfer fluid of systems such as a high-temperature nuclear fission reactor or a self-cooled nuclear fusion reactor needs to evaluate the behavior of tritium in Flinak and the permeability of tritium through Flinak facing metallic walls from the viewpoint of tritium safety. This is because radio-hazardous tritium will be produced in fusion reactors as well as in fission ones.

---

* Corresponding author. Tel.: +81 92 642 4140; fax: +81 92 642 3800.

E-mail address: sfukada@nucl.kyushu-u.ac.jp (S. Fukada).

0022-3115/$ - see front matter © 2006 Elsevier B.V. All rights reserved.
doi:10.1016/j.jnucmat.2006.07.011

Nomenclature

A	surface area, m^2
$c_{i,H}$	hydrogen concentration ($i = $ Ni or Flinak), mol-H/m^3 or mol-H_2/m^3
$D_{i,H}$	diffusivity of hydrogen ($i = $ Ni or Flinak), m^2/s
E	unspecified interaction energy between molten salt and gaseous molecules, J/mol
J_{H_2}	overall hydrogen permeation rate through a system of Ni and Flinak, mol-H_2/m^2s
K_{H_2}	Henry's solubility constant of H_2, mol/m^3Pa
K_{Henry}	Henry's solubility constant of gas, mol/m^3Pa
K_{Henry}^{Ost}	volumetric (Ostwald) solubility constant defined as $K_{Henry}R_gT$, –
L_i	thickness ($i = $ Ni or Flibe), m
N_A	Avogadro number, –
$p_{H_2,down}$	pressure of hydrogen at downstream side, Pa
$p_{H_2,up}$	pressure of hydrogen at upstream side, Pa
p_0	atmospheric pressure, Pa
P_{i,H_2}	permeability through $i = $ Ni or Flinak, mol-H/msPa$^{0.5}$ or mol-H_2/msPa
R_g	gas law constant, J/mol
r_b	radius of gas molecule determined from van-der-Waals equation of state, m
t	time, s
W	molar flow rate, mol/s
x	distance from Ni–H_2 interface, m
γ	surface tension, N/m

There are few data on permeability, diffusivity and solubility of hydrogen in Flinak except for Katsuta and Furukawa [7]. In addition, it is not clear whether or not hydrogen permeation obeyed diffusion-limiting condition in previous measurements. In the present study, the dependence of hydrogen permeation rate on the thickness of Flinak and on the upstream H_2 pressure was experimentally investigated. It will be clarified through the experiment whether or not the system is under the condition of diffusion-limiting permeation and what kinds of ions or molecular species are dissolved in Flinak and permeate through it. The solubility of hydrogen in Flinak is discussed in terms of macroscopic surface tension and the interaction energy between Flinak and gaseous molecules.

2. Experimental

Fig. 1 shows a schematic diagram of the experimental apparatus to determine the permeability, diffusivity and solubility of hydrogen in Flinak. A mixture of H_2 and Ar under a constant pressure and a constant flow rate was introduced into the bottom of a permeation vessel. The sidewall of the permeation vessel was made of 316 stainless-steel, and its outside wall was pretreated with heated air in order to decrease hydrogen permeation through it. Part of hydrogen was dissolved in an inside Ni bottom plate of 2.0 mm in thickness. Atomic hydrogen permeates through the Ni plate, and then ionic or bi-molecular hydrogen is dissolved in the molten Flinak. The thickness of Flinak was 20.0 mm or 40.0 mm. When hydrogen diffuses through Flinak including a certain amount of free fluorine ions, the chemical bonding is H^+–F^-. On the contrary, the bi-molecular form of H_2 is dissolved in Flinak under less free F^- ion conditions. When dissolved hydrogen has arrived at the upper interface between Flinak and Ar gas, hydrogen is swept away by an Ar purge flow. The Ar flow rate was maintained at 10 cm^3(NTP)/min. The H_2 concentration in the downstream Ar flow was detected by gas chromatography. The HF concentration was measured by a pH meter. The gas chromatography and the pH meter could detect H_2 with the sensitivity of 1 ppm and HF with that of 1 ppb, respectively. Another 316 stainless-steel vessel surrounded outside the permeation vessel. A space between the permeation vessel and the outside one was swept away by another Ar purge gas. Therefore, we neglected effects of by-pass hydrogen permeation through the sidewall. In addition, we needed to know how the interface between Flinak and Ar affects the overall H_2 permeation rate. In order to investigate the surface effect, the inlet was exchanged with the outlet. Then hydrogen permeated downward from the upper part through Flinak to the lower part. Results showed that overall permeation rates were

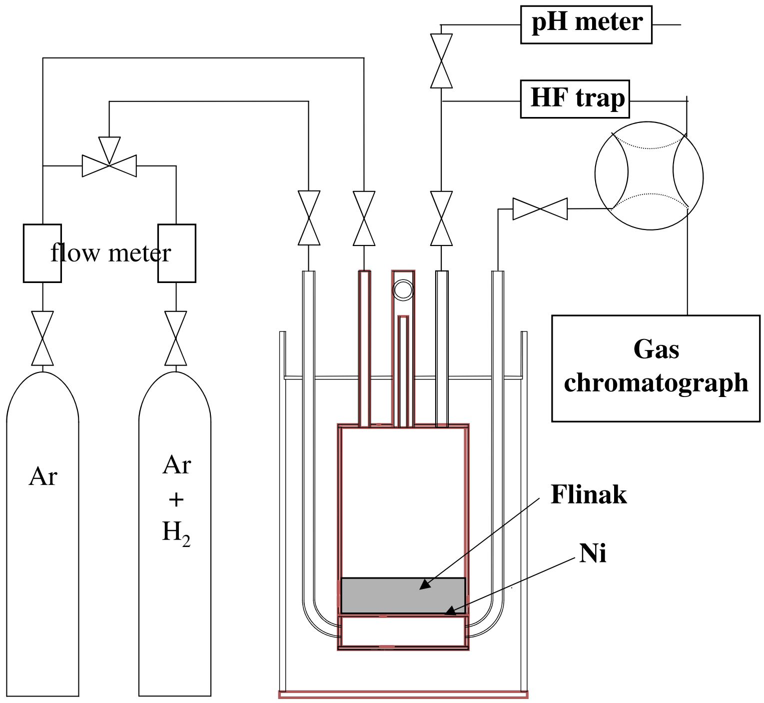

Fig. 1. A schematic diagram of the experimental apparatus to determine permeability, diffusivity and solubility of hydrogen in Flinak.

unchanged even when the direction of H_2 permeation was reversed. Therefore, it was concluded that the surface effect was negligibly small.

As a preliminary permeation experiment, we determined the rate of H_2 permeation through the Ni plate without Flinak. The H_2 permeability through the Ni plate was almost coincident with a reference that correlated a lot of previous Ni data [8]. Another experiment showed that Flinak does not corrode Ni [6]. Consequently, it was found that Ni worked as a good hydrogen permeation material regardless of its contact with Flinak. Before each Flinak permeation experiment, the upstream and downstream sides were purged by an Ar flow sufficiently. When the outlet H_2 concentration became zero, the upstream side was changed to an Ar + H_2 flow.

3. Analysis

The diffusion equation of a one-dimensional system comprising Ni and Flinak was described as follows:

$$\frac{\partial c_i}{\partial t} = D_{i,\mathrm{H}} \frac{\partial^2 c_i}{\partial x^2} \quad i = \mathrm{Ni\ or\ Flinak}. \tag{1}$$

Notation is given in the end of this text. The initial and boundary conditions were as follows:

$$t = 0, \quad c_{\mathrm{Ni}} = 0, \quad c_{\mathrm{Flinak}} = 0, \tag{2}$$

$$x = 0, \quad c_{\mathrm{Ni}} = c_{\mathrm{Ni},0}, \tag{3}$$

$$x = L_{\mathrm{Ni}}, \quad c_{\mathrm{Ni}} = c_{\mathrm{Ni,S}}, \quad c_{\mathrm{Flinak}} = c_{\mathrm{Flinak,S}}, \tag{4}$$

$$x = L_{\mathrm{Ni}} + L_{\mathrm{Flinak}}, \quad j_{\mathrm{H}_2} = -D_{\mathrm{Flinak,H}_2} \left.\frac{\partial c_{\mathrm{Flinak}}}{\partial x}\right|_{x=L_{\mathrm{Ni}}+L_{\mathrm{Flinak}}} = \frac{W_{\mathrm{down}} p_{\mathrm{H}_2,\mathrm{down}}}{A p_0}. \tag{5}$$

Flinak can absorb H_2 and HF depending on its reduction–oxidation (redox) condition. In this analysis, we assumed atomic dissolution (H) in Ni and bi-molecular dissolution (H_2) in Flinak. This assumption is discussed later based on comparison between experiment and calculation. When Flinak absorbs a dilute concentration of H_2, a Henry law is valid at the interface between molten Flinak and H_2 gas. Then, solubility is described as follows:

$$c_{\mathrm{Flinak,S}} = K_{\mathrm{H}_2} p_{\mathrm{H}_2,\mathrm{S}} \quad \text{at } x = L_{\mathrm{Ni}}, \tag{6a}$$

$$c_{\mathrm{Flinak,down}} = K_{\mathrm{H}_2} p_{\mathrm{H}_2,\mathrm{down}} \quad \text{at } x = L_{\mathrm{Ni}} + L_{\mathrm{Flinak}}. \tag{6b}$$

The above equilibrium relations should hold at the two interfaces between Flinak and Ni and between

Flinak and Ar. The H_2 permeability through Flinak, $P_{\mathrm{Flinak,H_2}}$, becomes a product of the diffusivity of H_2 in Flinak, $D_{\mathrm{Flinak,H_2}}$, and the solubility, $K_{\mathrm{H_2}}$, as follows:

$$P_{\mathrm{Flinak,H_2}} = D_{\mathrm{Flinak,H_2}} K_{\mathrm{H_2}}. \tag{7}$$

Fig. 2 shows a comparison of variations of the downstream H_2 partial pressure, $p_{\mathrm{H_2,down}}$, with time between experiment and calculation, when a constant H_2 partial pressure was maintained at the upstream side. The solid lines in the figure are ones determined by solving Eqs. (1)–(6) numerically. Close agreement was obtained between experiment and calculation using appropriate values of $D_{\mathrm{Flinak,H_2}}$ and $P_{\mathrm{Flinak,H_2}}$, while those of $D_{\mathrm{Ni,H}}$ and $P_{\mathrm{Ni,H}}$ were cited from the previous reference data [8].

The steady-state H_2 permeation rate, $(j_{\mathrm{H_2}})_{\mathrm{steady}}$, is reduced to Eq. (A.1) shown in the appendix. When the ratio of $P_{\mathrm{Flinak,H_2}}/L_{\mathrm{Flinak}}$ called a permeation resistance of Flinak is much smaller than that of $P_{\mathrm{Ni,H}}/2L_{\mathrm{Ni}}p^{0.5}_{\mathrm{H_2,down}}$ called a permeation resistance of Ni, the system is under diffusion-limiting condition. In other words, whether or not the system is diffusion-limiting depends on not only diffusivities of Ni and Flinak but also their thicknesses and hydrogen pressure. The steady-state rate of H_2 permeation through Flinak, $(j_{\mathrm{H_2}})_{\mathrm{steady}}$, under the diffusion-limiting condition is simplified to the following equation:

$$(j_{\mathrm{H_2}})_{\mathrm{steady}} = \frac{P_{\mathrm{Flinak,H_2}}}{L_{\mathrm{Flinak}}}(p_{\mathrm{H_2,up}} - p_{\mathrm{H_2,down}}). \tag{8}$$

For the diffusion-limiting permeation, some simplification of Eqs. (1)–(6) reduced the transient H_2 permeation rate, $j_{\mathrm{H_2}}$, to an analytical solution, Eq. (A.2), as also shown in Appendix A. The numerical solution to Eq. (1) under the conditions of Eqs. (2)–(6) was coincident with the analytical solution.

4. Results of hydrogen diffusivity and solubility in Flinak

4.1. Rate-determining step of overall H_2 permeation

Fig. 3 shows steady-state H_2 permeation rates, $(j_{\mathrm{H_2}})_{\mathrm{steady}}$, as a function of the upstream H_2 partial pressure, $p_{\mathrm{H_2,up}}$. It was apparent that $(j_{\mathrm{H_2}})_{\mathrm{steady}}$ was in proportion to $p_{\mathrm{H_2,up}}$ at 700 °C, because the downstream-to-upstream pressure ratio, $p_{\mathrm{H_2,down}}/p_{\mathrm{H_2,up}}$, was in the range of 1–5 × 10^{-4}. Thus, the linear pressure dependence of Eq. (8) was proved experimentally. The relation held even when the direction of H_2 permeation was changed from the top to the bottom. The result proved the preceding assumption that the hydrogen concentration at the interfaces between Flinak and Ar and between Flinak and Ni were in equilibrium. In other words, effects due to mass-transfer resistance across the interfaces were found to be negligibly small at 700 °C. However, there is a larger discrepancy from the linear

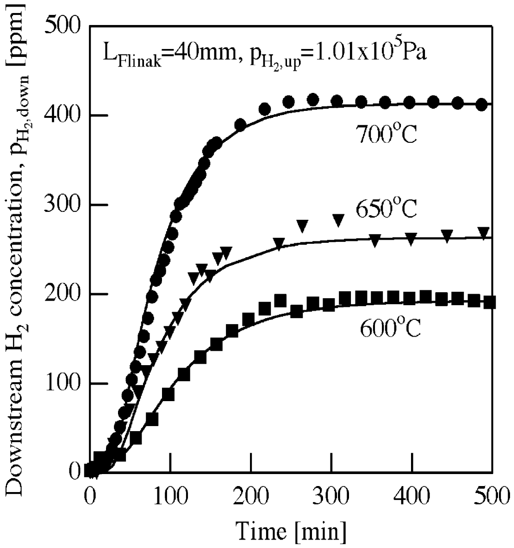

Fig. 2. Variations of downstream hydrogen concentration with time.

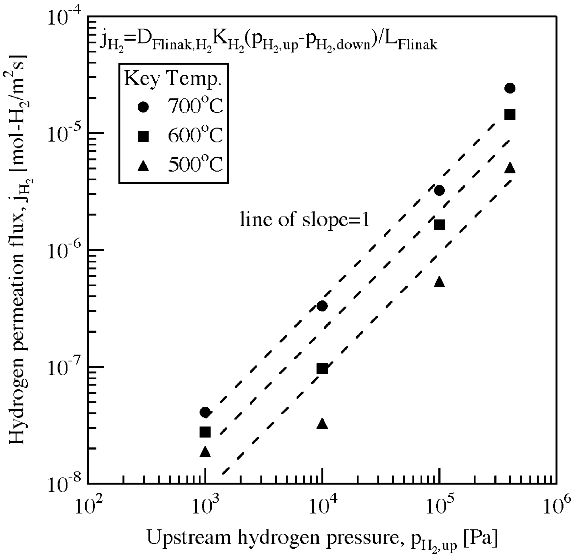

Fig. 3. Variations of steady-state H_2 permeation rate through Flinak with upstream H_2 partial pressure.

line for $(j_{H_2})_{steady}$ at 500 °C and 600 °C. This is because of the mass-transfer resistance across interfaces or impurities included in Flinak. Therefore, effects of H^+ ion diffusion seem to be present in the lower temperatures.

In addition to the above result, no HF was detected in the downstream Ar flow throughout the experiment. Therefore, it was probable that only H_2 permeated through Flinak.

Fig. 4 shows the dependence of $(j_{H_2})_{steady}$ on the thickness of Flinak, L_{Flinak}. As seen in the figure, it is apparent that $(j_{H_2})_{steady}$ is in reverse proportion to L_{Flinak}. These two experimental results lead to a fact that the system is under diffusion-limiting permeation, and a molecular form of H_2 permeates through Flinak.

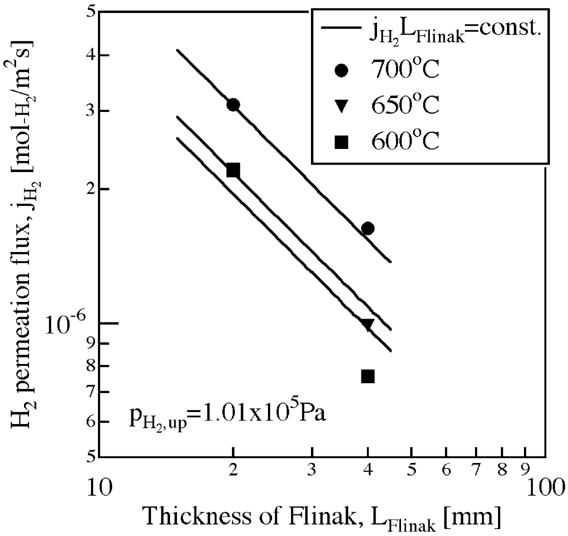

Fig. 4. Dependence of the steady-state rate of H_2 permeation through Flinak on thickness.

4.2. Diffusivity and solubility of H_2 in Flinak

Figs. 5 and 6 show the diffusivity and solubility of H_2 in Flinak as a function of the reciprocal of temperature, respectively. The slope of the solid line in Fig. 5 is −50 kJ/mol for H_2 diffusivity, and that in Fig. 6 is 34 kJ/mol for H_2 solubility. The diffusivity of H_2 in Flinak was correlated to the following equation:

$$D_{Flinak,H_2} = 8.69 \times 10^{-10} \exp\left(-\frac{50}{R_g T}\right)\ [m^2/s]. \tag{9}$$

The activation energy of D_{Flinak,H_2} for Flinak is smaller than that for Flibe [9] as comparatively shown in the figure. This may be because diffusion of hydrogen in Flibe is controlled by H^+ ion migration, and therefore it is strongly affected by its neighbor F^- ions. It was considered that the molecules of $2LiF + BeF_2$ in Flibe constitute a tetrahedral bond network of BeF_4^{2-} and Li^+ [9]. The network may raise the activation energy of H^+ diffusion through Flibe. On the other hand, H_2 migrates through ion pairs of Li^+–F^-, Na^+–F^- and K^+–F^- in Flinak. There seems to exist no definite bond network of Li^+–F^-, Na^+–F^- and

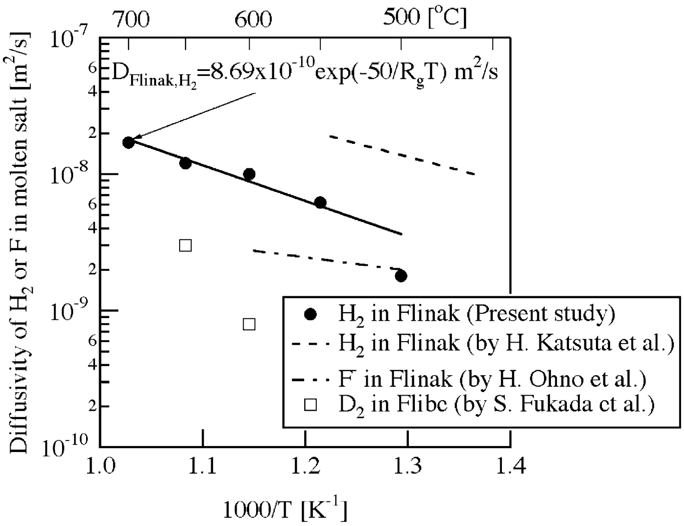

Fig. 5. Diffusivity of H_2 through Flinak as a function of the reciprocal of temperature.

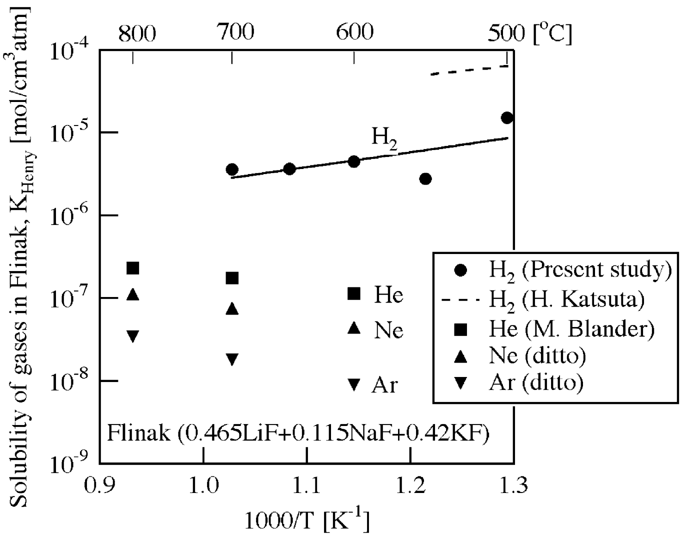

Fig. 6. Solubility of H_2 in Flinak as a function of the reciprocal of temperature.

K^+–F^-, and interaction with these ions is so small that the activation energy of H_2 diffusion in Flinak is smaller than that in Flibe.

The solubility of H_2 in Flinak, K_{H_2}, was correlated to the following equation:

$$K_{\text{Flinak},H_2} = 3.98 \times 10^{-7} \exp\left(\frac{34.4}{R_g T}\right) \quad [\text{mol/m}^3\ \text{Pa}]. \tag{10}$$

Its slope on the van't Hoff plot relates with absorption heat of hydrogen dissolved in Flinak, and the line with a positive slope means that the hydrogen absorption is exothermic. There is one-order magnitude difference in K_{Flinak,H_2} between Katsuta and Furukawa [7] (broken line) and ours (solid line). It is affected by impurities included in Flinak. This is because impurities in Flinak can change interaction energy between its neighbor molecules as discussed below. For comparison, solubilities of inert gases such as He, Ne and Ar in Flinak [10] are also shown in Fig. 6. Dissolution of several inert gases in Flinak was endothermic. The difference is discussed in terms of interaction energy in the following section.

5. Discussion on interaction energy between molten salt and dissolved gas

The solubilities of the inert gases obey the Henry law in a similar way to H_2. It is more advantageous to understand the solubilities of gases in the molten salt in terms of interaction energy between the salt and dissolved gas. The interaction energy was related with surface tension or other kinds of interaction [11]. Based on a usual solution theory [12], the Ostwald solubilities of gases in molten salts such as Flinak or Flibe were correlated to the following equation:

$$K^{\text{Ost}}_{\text{Henry}} = \exp\left[-\frac{E(T) + 4\pi N_A r_b^2 \gamma}{R_g T}\right] \quad [\text{mole/mole}]. \tag{11}$$

The molecules of H_2 and inert gases are localized at their respective equilibrium positions among molten salt ions. The position relates with attractive or repulsive interaction force imposed from its neighbor ions that comprise molten salts. As the first approximation, the overall interaction energy is determined as the summation of a repulsive macroscopic surface tension, $4\pi N_A r_b^2 \gamma$ [15] and a repulsive or attractive interaction energy of $E(T)$.

Fig. 7 shows E values for He, Ne and Ar [10] in Flinak as well as that for H_2. In addition, E values for He, Ne, Ar, Xe [13] and H_2 [9,11] in Flibe are shown in the figure. As seen in the figure, the E values for He, Ne and Ar were independent of the kind of the molten salts (Flibe and Flinak) as well as temperature. Its value was 13.6 kJ/mol for He, Ne and 9.9 kJ/mol for Ar. Thus, the E values of inert gases except for Xe were positive, and therefore the interaction was repulsive. The H_2 solubility in Flibe

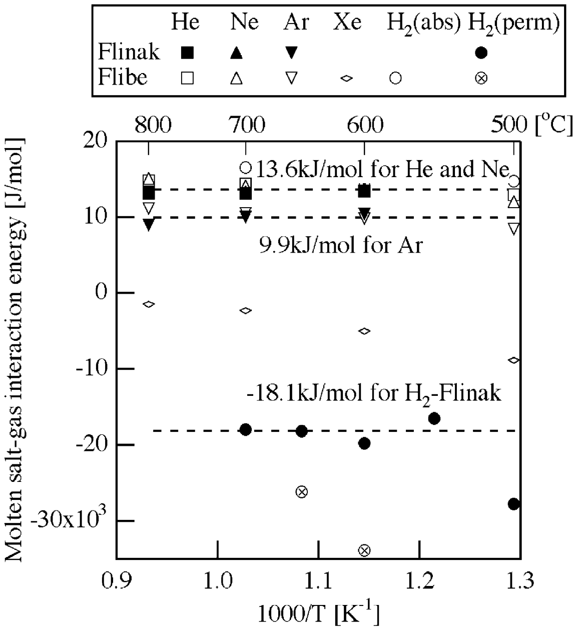

Fig. 7. Interaction energy between molten salts and gases.

purified by HF [11,13] was also the same as the He one, and the E value was 13.6 kJ/mol. On the other hand, the E value for the present H_2-Flinak system was -18.1 kJ/mol, and that for the H_2–Flibe system [9] was around -30 kJ/mol. The negative energy means that the interaction is attractive. There was a difference between the H_2 solubility determined from H_2 permeability [9] and that from the absorption experiment [11]. The former was hundreds-fold higher than the latter and was almost the same as the HF solubility in Flibe [14]. There may be two explanations for the difference in H_2 capacity; (1) contribution of HF and (2) effects of impurities. Free F^- ions and metallic impurities can chemically combine with dissolved H^+ ions resulting in an increase of the H^+ capacity in Flibe and Flinak. This increase may cause a time delay to reach a steady-state H_2 permeation rate. On the other hand, the effect of dissolved H^+ ion may be small when Flibe was purified by HF before the H_2 absorption experiment. The increase in apparent H_2 solubility may result in the large change of $E(T)$.

6. Conclusions

Permeability, diffusivity and solubility of H_2 in Flinak molten salt were determined. The H_2 permeability through Flinak had almost linear pressure dependence and was in reverse proportion to the thickness of Flinak. Therefore, the system was under diffusion-limiting permeation and hydrogen permeated through Flinak as H_2. The H_2 diffusivity through Flinak was correlated to the relation of $D_{\mathrm{Flinak,H_2}} = 8.69 \times 10^{-10} \exp(-50/R_gT)$ [m^2/s]. The H_2 solubility in Flinak was correlated to the Henry law, and its solubility was correlated to a thermodynamic relation in terms of Eq. (11) as well as other inert gas solubility. The interaction energy between H_2 and Flinak was an attractive one of 18.1 kJ/mol and those for inert gases were repulsive ones of 9.9–13.6 kJ/mol. The interaction energy between Flinak and dissolved gas was almost the same between Flibe and dissolved gas.

Acknowledgments

This study was financially supported partially by the NIFS coordinate research (Contract number NIFS04KFDS001) and partially by Ministry of Education, Science, Sports and Culture, Grant-in-Aid for Exploratory Research, 2005, 17656297. The authors appreciate useful discussion with members of Japan–USA Program for Irradiation/Integration Test for Fusion Research-II (JUPITER-II), task 1-1-A Flibe/tritium chemistry group.

Appendix A. Simplification of Eqs. (1)–(6) for the transient or steady-state hydrogen permeation through the Ni and Flinak system

With the assumptions of atomic dissolution in Ni and bi-molecular dissolution in Flinak, the steady-state H_2 permeation rate, $(j_{H_2})_{\mathrm{steady}}$, is reduced to the following equation:

$$(j_{H_2})_{\mathrm{steady}} = \frac{\left[\left(\frac{L_{\mathrm{Flinak}}}{P_{\mathrm{Flinak,H_2}}} + \frac{2\sqrt{p_{\mathrm{H_2,down}}}L_{\mathrm{Ni}}}{P_{\mathrm{Ni,H}}}\right)^2 + 4\left(\frac{L_{\mathrm{Ni}}}{P_{\mathrm{Ni,H}}}\right)^2 (p_{\mathrm{H_2,up}} - p_{\mathrm{H_2,down}})\right]^{0.5} - \left(\frac{L_{\mathrm{Flinak}}}{P_{\mathrm{Flinak,H_2}}} + \frac{2\sqrt{p_{\mathrm{H_2,down}}}L_{\mathrm{Ni}}}{P_{\mathrm{Ni,H}}}\right)}{2\left(\frac{L_{\mathrm{Ni}}}{P_{\mathrm{Ni,H}}}\right)^2}. \tag{A.1}$$

When H_2 diffusion through Flinak is rate-determining, *i.e.*, $L_{\mathrm{Flinak}}/P_{\mathrm{Flinak,H_2}} \gg 2p^{0.5}_{\mathrm{H_2,down}}L_{\mathrm{Ni}}/P_{\mathrm{Ni,H}}$, Eq. (A.1) can be reduced into Eq. (8) in the text.

On the other hand, an analytical solution to Eq. (1) for the transient H_2 permeation through Flinak under the diffusion-limiting permeation is expressed as follows:

$$\frac{j_{\mathrm{H_2}}L_{\mathrm{Flinak}}}{D_{\mathrm{Flinak,H_2}}K_{\mathrm{H_2}}(p_{\mathrm{H_2,upstream}}-p_{\mathrm{H_2,downstream}})} = 2\sqrt{\frac{L^2_{\mathrm{Flinak}}}{\pi D_{\mathrm{Flinak,H_2}}t}}\sum_{n=1}^{\infty}\exp\left[-\frac{(2n-1)^2L^2_{\mathrm{Flinak}}}{4D_{\mathrm{Flinak,H_2}}t}\right]. \tag{A.2}$$

The steady-state H_2 flux in the downstream side, $j_{\mathrm{H_2}}$, gives information on a product of $D_{\mathrm{Flinak,H_2}}K_{\mathrm{H_2}}$ based on the left-hand side of (A.2), and the change of the transient hydrogen flux gives information on $D_{\mathrm{Flinak,H_2}}$ based on the right-hand side of (A.2).

References

[1] H.W. Hoffman, CF-53-8-106, ORNL Technical Report, 1953.

[2] J. Braunstein, G. Mamantov, G.P. SmithAdvanced in Molten Salt Chemistry, vol. 3, Plenum, New York, 1975, p. 386.

[3] S.R. Sherman, 2005 DOE hydrogen program: NHI system interface and support system, 2005 DOE H_2 Annual Review, Project ID #PD31.

[4] S. Fukada, M. Nishikawa, A. Sagara, Fus. Technol. 39 (2001) 1073.

[5] S. Fukada, M. Nishikawa, A. Sagara, Fus. Sci. Technol. 41 (2002) 1054.

[6] S. Fukada, A. Morisaki, A. Sagara, T. Terai, Fus. Eng. Des. 81 (2006) 477.

[7] H. Katsuta, K. Furukawa, Rev. Chim. Miner. 15 (1978) 49.

[8] W.M. Robertson, Z. Metallde. 64 (1973) 436.

[9] S. Fukada, R.A. Anderl, A. Sagara, M. Nishikawa, Fus. Sci. Technol. 48 (2005) 666.

[10] M. Blander, W.R. Grimes, N.V. Smith, G.M. Watson, J. Phys. Chem. 63 (1959) 1164.

[11] A.P. Malinauskas, D.M. Richardson, Ind. Eng. Chem. Fundam. 13 (1974) 242.

[12] J.O. Hirshfelder, C.F. Curtiss, R.B. Bird, Molecular theory of gases and liquids, Wiley, 1954.

[13] G.M. Watson, R.B. Evans, W.R. Grimes, N.V. Smith, J. Chem. Eng. Data 7 (1962) 285.

[14] P.E. Field, J.H. Shaffer, J. Phys. Chem. 71 (1967) 3218.

[15] H. Ono, T. Omichi, K. Furukawa, JAERI-M-4750 (1972), original data are present in ORNL-3591, 1964.